ORIGINAL PAPER

The influence of different variables on the electrochemical behavior of mild steel in circulating cooling water containing aggressive anionic species

M. A. Deyab

Abstract Cyclic voltammetric, potentiodynamic anodic polarization and current–time transient studies were carried out on mild steel in circulating cooling water containing Cl^- and SO_4^{-2} ions under the effect of different variables such as coolant flow, the availability of oxygen, cooling system temperature, and cooling system pH. The anodic excursion span of mild steel in cooling corrosive solution was characterized by the occurrence of a well-defined anodic peak (A1), while the reverse sweep was characterized by the appearance of two cathodic peaks (C1 and C2). The presence of Cl^- and SO_4^{-2} ions in cooling water enhance the active dissolution of mild steel and tend to breakdown the passive film and induce pitting attack. The data reveal that increasing flow rate and temperature of cooling solution enhances the anodic peak current density (j_{A1}) and shifts the pitting potential (E_{pit}) towards more active values. It is seen that the peak current density of the anodic peak A1 increases and the pitting potential (E_{pit}) displaced in the noble direction in the aerated solution compared that in de-aerated solution. The pitting corrosion of mild steel by Cl^- and SO_4^{-2} ions initiates more readily in acidic medium (pH 2.0). It was found that the incubation time (t_i) increase and in turn the pitting corrosion decrease in the order: pH 10>pH 6.8>pH 2.0.

Keywords Mild steel · Cooling water · Pitting corrosion · Polarization

M. A. Deyab (✉)
Egyptian Petroleum Research Institute (EPRI),
Nasr City,
Cairo, Egypt
e-mail: hamadadeiab@yahoo.com

Introduction

Most automotive and diesel engines require cooling systems using circulating water. The cooling medium may remain in use for month at time. The function of the cooling system of an internal combustion engine is to transfer heat from the engine to the radiator where the heat can be dissipated to the air. Anything that interferes with the proper function of the system can have a harmful effect on engine performance. Since the corrosion of cooling system metals can lead to the malfunction of the parts and cause excessive corrosion of ferrous metal parts in a few months of car service [1–3], it is very important that careful attention be paid to study the corrosion behavior of cooling system metal at different variables. The presences of chloride and sulfate ions in circulating water are particularly aggressive and accelerate corrosion [4, 5].

In the present study, aspects of electrochemical behavior of mild steel in circulating cooling water containing chloride and sulfate ions were investigated potentiodynamically and galvanostatically. In addition, the effect of many variables on the cooling corrosion like coolant flow, the availability of oxygen, cooling system temperature, and cooling system pH were also studied.

The experimental details

For electrochemical measurements, the newly designed water-jacketed electrolytic cell was used (Fig. 1). It was made of Pyrex glass without any rubber connections.

Mild steel specimen having chemical compositions 0.15% C, 0.18% Si, 0.27% Mn, 0.03% P, 0.014% S, the remainder being Fe, and having an exposed area of 0.672 cm^2 was used as a working electrode. The specimens were mechanically polished using different grades of emery

Fig. 1 Schematic diagram of the electrochemical cell
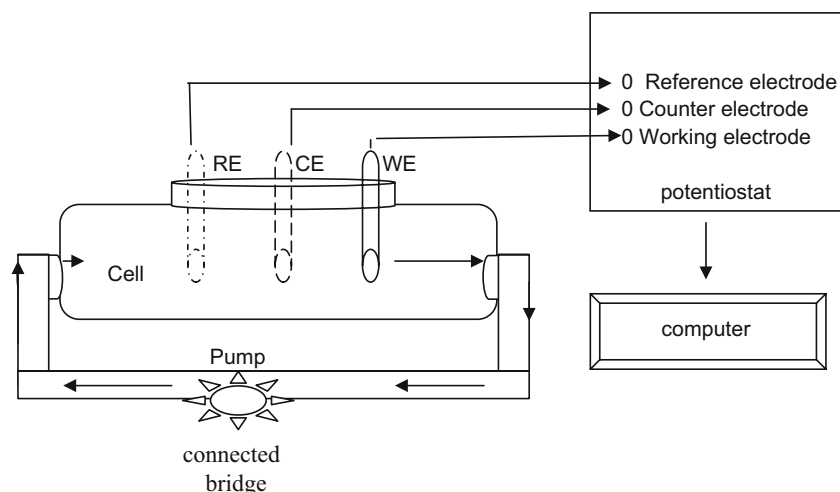
paper (120, 400, 800, 1,000, and 1,200), washed thoroughly with distilled water, and degreased with acetone. The cell assembly consisted of mild steel as working electrode, a platinum foil as counter electrode, and a saturated calomel electrode (SCE) as a reference electrode.

The potentiodynamic current–potential curves were recorded using a potentioscan type (potentiostat/galvanostat EG&G model 273) connected with a personal computer. Potentiodynamic E/j were carried out by changing linearly the electrode potential automatically from the starting potential (−2.0 V versus SCE) towards more positive direction with a required scan rate until the end of the experiment.

The potentiostatic current/time transients (chronoamperometry) were recorded for mild steel electrode in test solution at a constant anodic potential ($E_{s,a}$). When performing the potentiostatic j/t transients, the measurements were carried out after a two-step procedure, namely: the working electrode was first held at the starting potential (−2.0 V) 60 s to attain a reproducible electroreduced electrode surface. Then the electrode was polarized in the positive direction to a step anodic potential $E_{s,a}$ at which the anodic current transient was recorded.

For experiments in de-aerated environments, the electrode was immersed after the solution was purged with pure nitrogen for 10 min and the solution was kept purged above the solution until the end of the experiment.

The solutions were prepared using analytical reagent-grade chemicals and double-distilled water. The test solution was prepared by dissolving 100 ppm NaCl and 100 ppm Na_2SO_4 in double-distilled water. The pH of the solution was adjusted at pH 2, 6.8, and 10 using hydrochloric acid and sodium hydroxide. During the preparation of the solution at pH 2 using hydrochloric acid, the amount of NaCl was adjusted to maintain the chloride ion concentration constant. The volume of the test solution was 1,000 ml. A Lseibolo Wien pH meter was used to measure

the pH values for all prepared solutions. Nissan water pump (NWP) was used to increase the solution flow rate inside the electrolytic cell (from 0 to 1.66 m s^{-1}). The temperature (from 25 to 65 °C) was adjusted to within ±0.2 °C using a water thermostat.

Results and discussion

Effect of cooling corrosive solution

Representative cyclic voltammogram of mild steel in aerated cooling corrosive solution (100 ppm Cl^{-}+100 ppm SO$_4^{-2}$ dissolved in distilled water, pH=6.8) over a wide potential range and at 25 °C with scan rate of 5 mV s^{-1} was shown in Fig. 2. The potentiodynamic trace in the anodic direction
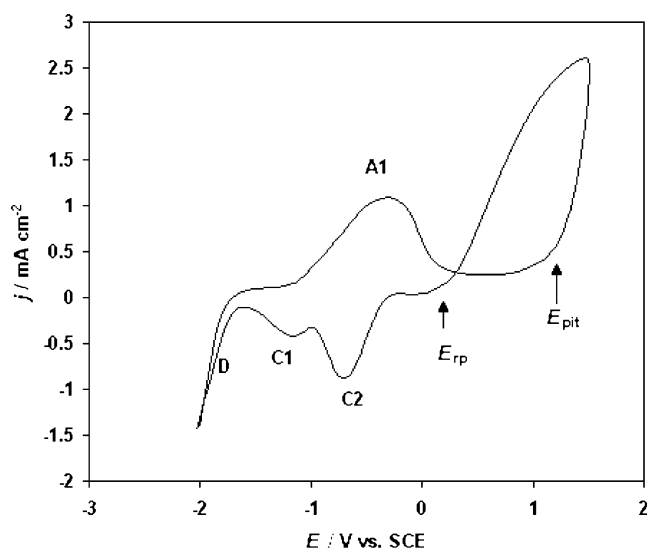

Fig. 2 Cyclic voltammogram of mild steel in aerated cooling solution (100 ppm Cl^{-}+100 ppm SO$_4^{-2}$, pH=6.8) at 25 °C with scan rate of 5 mV s^{-1}

displays an anodic active dissolution peak A1 with a peak current of 1.14 mA cm^{-2} at −0.34 V. Peak A1 represents active dissolution of the mild steel as Fe (II) [6]. It is observed that at a certain critical potential (pitting potential E_{pit}=1.2 V), the anodic current density increases steeply without any sign for oxygen evolution. The rapid rise in anodic current density at E_{pit} indicates initiation and growth of pitting attack. The pitting corrosion could be related to the ability of the Cl$^-$ and SO$_4^{-2}$ anions to adsorb on the passive film and create an electrostatic field across the film/electrolyte interface [7]. When the field reaches a certain value, the adsorbed anions penetrate the oxide film especially at the flaws and defects in the oxide film [8]. When the penetrated Cl$^-$ and SO$_4^{-2}$ anions reach the metal surface, they promote local anodic dissolution resulting in a pit nucleus. Following this, a pit growth takes place rapidly because of an increase in corrosive ion concentration resulting from its migration, and increases the acidity inside the pits [9]. When the potential limit is reversed, the pitting current exhibits a hysteresis loop and decreases rapidly reaching zero at a certain repassivation potential (E_{rp}= 0.13 V) when all growing pits become repassivate. The repassivation process could be achieved by removal of accumulated Cl$^-$ and SO$_4^{-2}$ ions from the pits by diffusion [10]. On the other hand, the cathodic sweep shows two cathodic peaks C1 at potential −1.19 V and C2 at potential −0.75 V. The cathodic peak C1 is probably in conjugation to the anodic peak A1 and could be attributed to reduction of oxide formed during the potential scan at −0.34 V. The cathodic peak C2 is most likely due to the reduction of pitting corrosion product formed during the potential scan at $E \geq 1.2$ V. The large cathodic current (D), which was observed when the potential was further decreased after the cathodic peak C1 is due to the hydrogen reduction and evolution of hydrogen gas.

The effect of increasing aerated cooling solution flow rate (from 0 to 1.66 m s^{-1}) on the potentiodynamic anodic polarization behavior of mild steel with scan rate of 5 mV s^{-1} was examined between E_c=−2.0 V and E_a=1.5 V at 25 °C and the data were represented in Fig. 3. The effect of solution flow rate on E_{pit} and j_{A1} derived from Fig. 3 has been represented in Fig. 4. Inspection of the data reveals that increasing flow rate increases the anodic current density peak j_{A1}. At the same time, the anodic potential peaks, E_{A1}, were shifted to more noble values. It is clear that the rate of movement of the cooling solution with respect to the mild steel is a major factor in the corrosion of metals. The accelerating effect results from the higher rate at which the corrosive Cl$^-$ and SO$_4^{-2}$ ions are brought to the corroding surface and corrosion products (which might otherwise accumulate and stifle corrosion) are carried away. The higher the velocity, the thinner will be the quiescent layers of the metal surface
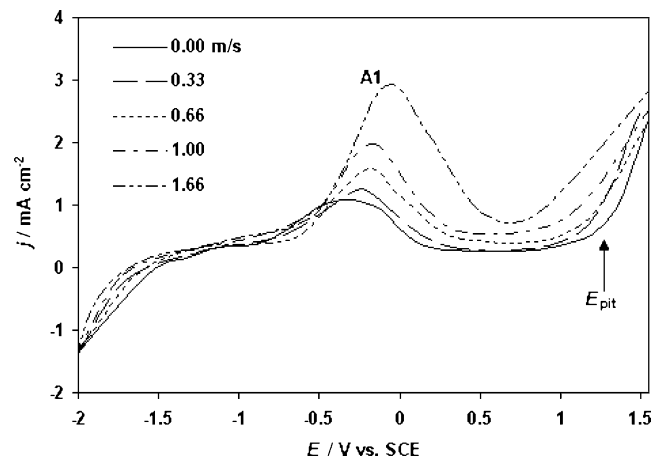

Fig. 3 The effect of aerated cooling solution flow rate on the potentiodynamic anodic polarization curves of mild steel at 25 °C with scan rate of 5 mV s^{-1}

through which corroding substances like rust penetrate and through which soluble corrosion products must diffuse [11]. It is clear also that the values of E_{pit} move in the active direction, with increase in flow rate from zero to 1.66 m s^{-1}. The decrease in E_{pit} with increase in flow rate may be attributed to the increased ionic activity of Cl$^-$ and SO$_4^{-2}$ ions or their collective synergistic effects.

Effect of temperature

Potentiodynamic anodic polarization curves for mild steel in naturally aerated cooling solution at scan rate of 5 mV s^{-1} with solution flow rate of 0.66 m s^{-1} for different solution temperatures are shown in Fig. 5. The effect of solution temperature on E_{pit} and j_{A1} derived from Fig. 5 has been represented in Fig. 6. Increasing the solution temperature from 25 to 65 °C was found to increase the peak current density of the anodic peak A1 and shifted their peak potentials towards more positive values. This behavior could
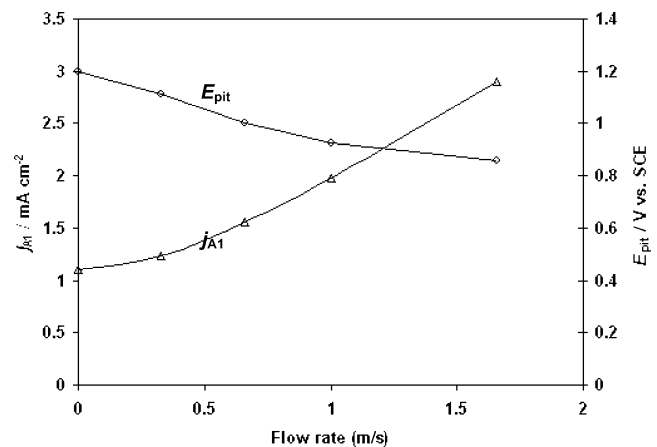

Fig. 4 Relation between E_{pit} and j_{A1} versus cooling solution flow rate
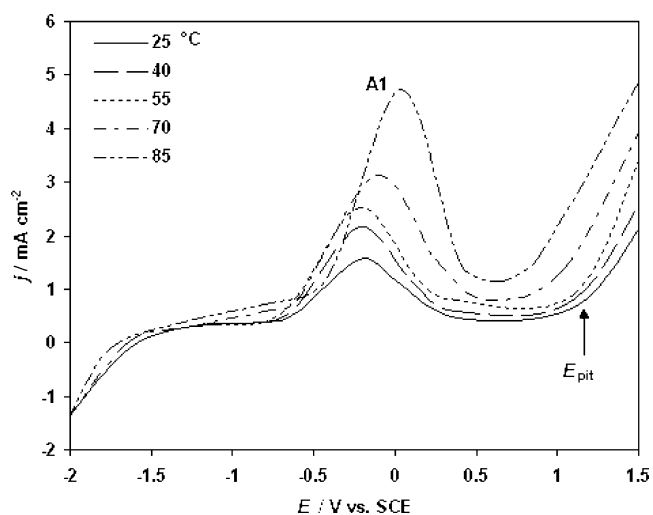
Fig. 5 The effect of aerated cooling solution temperature on the potentiodynamic anodic polarization curves of mild steel at scan rate of 5 mV s^{-1} and with flow rate of 0.66 m s^{-1}

be attributed to the increase in the diffusion coefficient of the diffusive species with increasing the solution temperature [12] where the diffusion coefficient (D) is related to the peak current density via the Randles–Sevcik [13] equation:

$$j_A \; \alpha \; D^{1/2} \tag{1}$$

It was found also that solution temperature has a pronounced effect on E_{pit} values. The E_{pit} decreased with increase in temperature, indicating that mild steel is more prone to pitting corrosion at higher temperatures up to 65 °C. Such effect of temperature on pitting corrosion of mild steel may be attributed to an increase in solubility of oxide film with temperature. In addition, an increase in temperature accelerates the rates of diffusion and migration of the reactant and product species [14, 15].
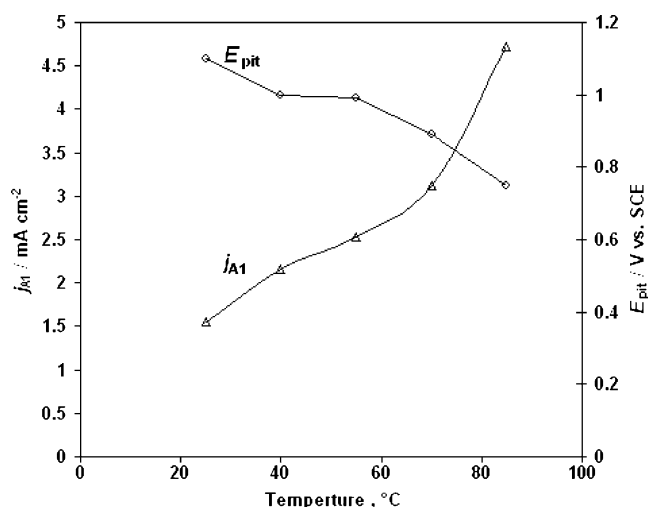

Fig. 6 Relation between E_{pit} and j_{A1} versus cooling solution temperature

Effect of de-aerated environment

Figure 7 shows potentiodynamic anodic polarization curves of mild steel electrode in aerated and de-aerated cooling solution (pH=6.8) over a wide potential range and at 25 °C with flow rate of 0.66 m s^{-1}. In the aerated solution, the anodic pack potential (A1) was −0.22 V with a small passive region with its average current density of 0.41 mA cm^{-2}, extending from 0.38 to 1.1 V, where passive layer breakdown takes place due to the pitting corrosion. In the aerated solution, the cathodic reaction is oxygen reduction according to [16],

$$2O_2 + H_2O + 2e- \rightarrow 2OH^- \tag{2}$$

In the de-aerated cooling solution, the anodic pack potential (AI) became more negative at −0.451 V with the current of 0.45 mA cm^{-2} in the passivation region, where the cathodic reaction should be water reduction according to [16]

$$2H_2O_{(S)} + 2e^- \rightarrow H_2 + 2OH^- \tag{3}$$

It is seen that the peak current density of the anodic peak A1 increases and its peak potential moves towards more positive value in the aerated solution compared that in aerated solution. It clear also that anodic current increase continuously in the passive region with the pitting potential E_{pit} shifting in a more negative direction in the de-aerated solution compared to that in the aerated solution. This is due to the lack of O_2 in the solution, which is necessary to increase the thickness of the oxide film [17].

The chronoamperograms for the mild steel electrode in aerated and de-aerated cooling solution (pH=6.8) with flow rate of 0.66 m s^{-1} at 25 °C are illustrated in Fig. 8. Chronoamperometric curves recorded for 20 min at 567 mV,

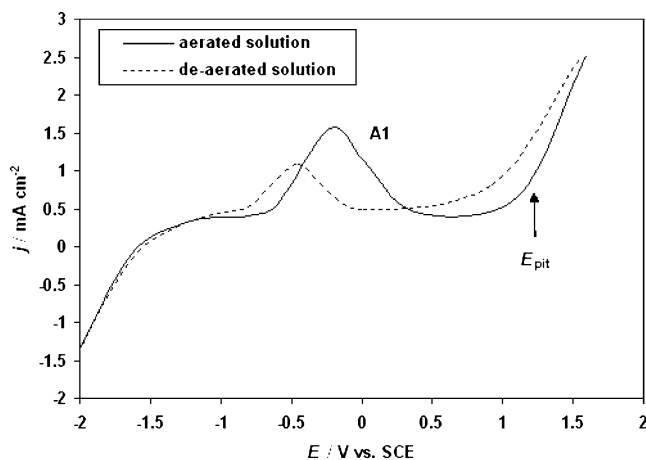**Fig. 7** Potentiodynamic anodic polarization curves of mild steel electrode in aerated and de-aerated cooling solution (pH=6.8) at 25 °C and at scan rate of 5 mV s^{-1} and with flow rate of 0.66 m s^{-1}
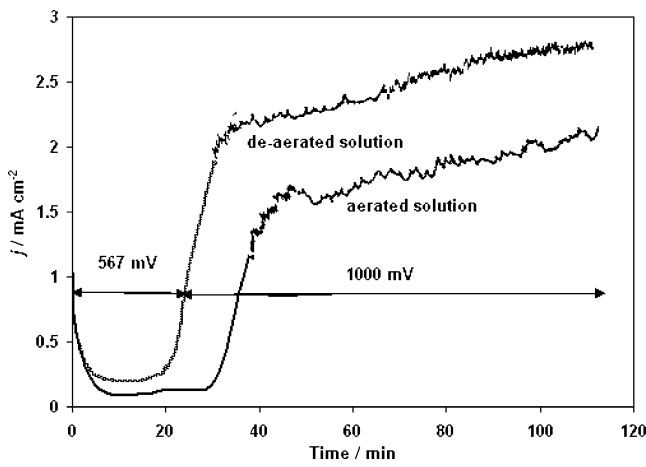
Fig. 8 Current–time curves for the mild steel electrode in aerated and de-aerated cooling solution (pH=6.8) with flow rate of 0.66 m s^{-1} at 25 °C

where a thick oxide film would have been formed on the metal surface, and then the potential was stepped at 1,000 mV for 110 min. At 1,000 mV, the passive layer breakdown would take place in aerated and de-aerated cooling solution. It was found that in de-aerated cooling solution, the large current increase at a certain incubation time (t_i) followed by fluctuations was observed due to the occurrence of both initiation and propagation of pitting corrosion [18, 19], which was seen to be significantly suppressed in the aerated cooling solution. The incubation time is caused by the time required for local removal of the passive film via the sequence of corrosive ions adsorption, penetration, and formation of a readily soluble complex. The data infer that the pitting growth current density increases and the incubation time become shorter and hence the rate of pit growth increases, in the de-aerated solution compared to that in the aerated solution. These results agree with the results obtained from potentiodynamic measurements.
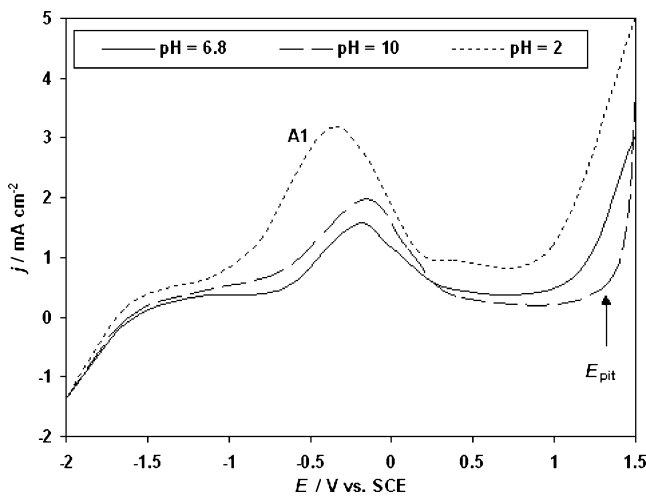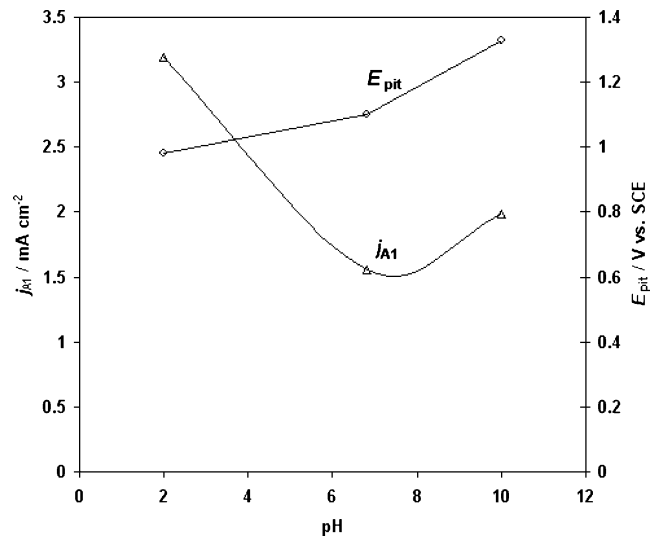

Fig. 10 Relation between E_{pit} and j_{A1} versus cooling solution pH

Effect of cooling solution pH

The effect of pH of the cooling solution adjusted at values of 2.0, 6.8, and 10 on the potentiodynamic anodic polarization curves of mild steel electrode in aerated environment at 25 °C with flow rate of 0.66 m s^{-1} are presented in Fig. 9. The effect of solution pH on E_{pit} and j_{A1} derived from Fig. 9 has been represented in Fig. 10. The main feature in the curves is that the highest value of anodic current density of peak A1 (j_{A1}) is at pH 2.0, while the lowest one is at pH 6.8. These results may be due to an increase in the solubility in both acidic (pH 2.0) and alkaline (pH 10) media [20]. It seems that the passivity regions are pH dependent. It is notable that the highest value of E_{pit} is at pH 10, while the lowest value is at pH 2.0. This indicates that mild steel in cooling solution system is more susceptible to pitting corrosion in acidic medium. On the other

Fig. 9 The effect of pH of the cooling solution on the potentiodynamic anodic polarization curves of mild steel electrode in aerated solution at 25 °C with flow rate of 0.66 m s^{-1} and at scan rate of 5 mV s^{-1}

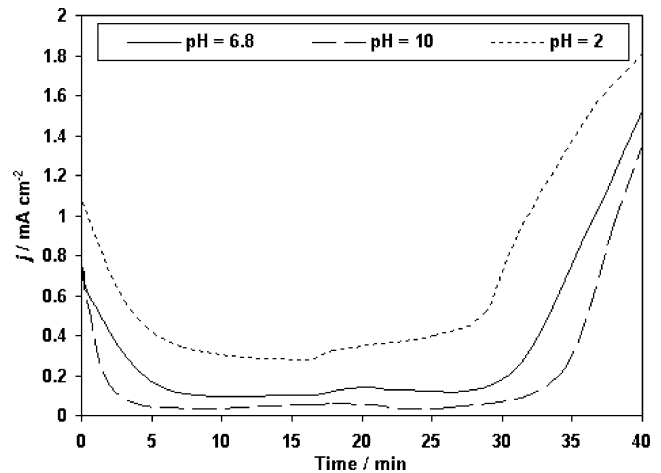**Fig. 11** Current–time curves for the mild steel electrode in aerated cooling solution at 25 °C with flow rate of 0.66 m s^{-1} at different pH values

hand, the resistance of mild steel to pitting corrosion is higher in alkaline solution (pH 10). This behavior could be attributed to the type of charge in the metal surface at different pH [21]. At pH 2.0, the metal surface is probably positively charged, while at pH 10 it is negatively charged. The Cl^- and SO_4^{-2} anions will be directly attached to the positively charged surface, which led to a shift in the pitting potential E_{pit} to a more negative value [22]. On the other hand, at pH 10, protonated water will adsorb on the negatively charged surface, giving rise to passive conditions, when conditions favor formation of hydroxide precipitate [23]. This explains the shift of E_{pit} towards the noble direction at pH 10.

The effect of the cooling solution pH on the current/time transient for mild steel electrode with flow rate of 0.66 m s^{-1} at 25 °C were recorded for 40 min at 1,000 mV in Fig. 11. The data infer that the current density decreases with time reaching quasi-steady state current values. In this case, the transient current is related to nucleation and growth of ferrous oxide passive layer. The figure shows that at all pH values the transient current density initially decreases to a minimum value at a certain incubation time (t_i) and then increases. The general trend of an increasing current suggests that pit growth is the dominant process and a number of well-developed pits. Data reveal that the incubation time (t_i) is pH dependent. Incubation time increases in the order: pH 10>pH 6.8>pH 2.0. This indicates that the time required for local removal and breakdown of the passive film by Cl^- and SO_4^{-2} ions is longer in alkaline medium. These results agree with the results obtained from potentiodynamic measurements.

Summary

The present study has investigated the electrochemical behavior of mild steel in circulating water containing chloride and sulfate ions. In addition, the influence of major factors, which affect pitting corrosion such as coolant flow, the availability of oxygen, cooling system temperature, and cooling system pH.

The following conclusions can be drawn from the results obtained.

1. The appearance of one anodic peak A1 and two cathodic peaks (C1 and C2) characterized the cyclic voltammetric response. The presence of hysteresis loop in the curve is also clear due to pitting corrosion.
2. The data reveals that increasing flow rate from 0 to 1.66 m s^{-1} increases the anodic current density peak j_{A1} and moves the E_{pit} value in the active direction.
3. The increasing of the cooling solution temperature increases the general and pitting corrosion of mild steel.
4. The data obtained for potentiodynamic and chronoamperometric measurements infer that the pitting corrosion of mild steel is more pronounced in de-aerated solution than that in the aerated solution.
5. The polarization data indicated that the highest values of anodic current density of peak A1 (j_{A1}) is at acidic medium (pH 2.0), while the lowest one is at natural medium (pH 6.8). On the other hand, the current–time transient data show that the incubation time increases and hence, the rate of pit growth decreases in the order: pH 10>pH 6.8>pH 2.0.
6. In conclusion, the presence of Cl^- and SO_4^{-2} ions in acidic de-aerated circulating cooling water with increasing solution temperature and flow rate can have a harmful effect on engine performance.

References

1. Mor ED, Wrbbl C (1976) Br Corros J 11:199
2. Vanloyen D, Zucher G (1990) Werkst Korros 11:613. doi:10.1002/maco.19900411103
3. Singh IB, Venkatachari G, Balarishman K (1994) J Appl Electrochem 24:197
4. Marco JF, Gancedo JR, Meisel N, Griesbach P, Gütlich P (1991) Corros 47:498
5. Bird HEH, Pearson BR, Brook PA (1988) Corros Sci 28:81. doi:10.1016/0010-938X(88)90009-1
6. Lorenz WJ, Heusler KE (1987) Corrosion mechanisms. Marcel Dekker, New York
7. Szklarska-Smialowska Z (1986) Pitting corrosion of metals. NACE, Houston
8. Aramaki K, Shimura T (2006) Corros Sci 48:2009
9. Brett CMA (1990) J Appl Electrochem 20:1000. doi:10.1007/BF01019579
10. Foad El-Sherbini EE, Abd-El-Wahab SM, Amin MA, Deyab MA (2006) Corros Sci 48:1885. doi:10.1016/j.corsci.2005.08.002
11. Lu Q, Stack MM, Wiseman CR (2001) J Appl Electrochem 31:1373. doi:10.1023/A:1013824010279
12. Zaky AM, Abd El Rehim SS, Mohamed BM (2006) Int J Electrochem Sci 1:17
13. Randles JEB (1948) Trans Faraday Soc 44:327. doi:10.1039/tf9484400327
14. Abd El Meguid EA, Mahmoud NA, Gouda VK (1998) Br Corros J 33:42
15. Almarshad AI, Jamal D (2004) J Appl Electrochem 34:67. doi:10.1023/B:JACH.0000005579.84264.73
16. Badawy WA, Al-Kharafi FM, El-Azab AA (1999) Corros Sci 41:709. doi:10.1016/S0010-938X(98)00145-0
17. Sherif EM, Park Su-Moon (2006) Electrochim Acta 51:1313. doi:10.1016/j.electacta.2005.06.018
18. Stewart J, Balkwill PH, Williams DE (1994) Corros Sci 36:1213. doi:10.1016/0010-938X(94)90145-7
19. Frankel GS (1998) J Electrochem Soc 45:2186. doi:10.1149/1.1838615
20. Ambat R, Dwarakadasa ES (1994) J Appl Electrochem 24:911. doi:10.1007/BF00348781
21. Mazhar AA, Arab ST, Noor EA (2001) J Appl Electrochem 31:1131. doi:10.1023/A:1012039804089
22. Parks GA (1965) Chem Rev 65:177. doi:10.1021/cr60234a002
23. Tomcsányi L, Varga K, Bartik I, Horányi H, Maleczki E (1989) Electrochim Acta 34:855. doi:10.1016/0013-4686(89)87119-1